Bioorganic & Medicinal Chemistry Letters 23 (2013) 4627–4632

Contents lists available at SciVerse ScienceDirect

Bioorganic & Medicinal Chemistry Letters

journal homepage: www.elsevier.com/locate/bmcl

Discovery and optimisation of 1-hydroxyimino-3, 3-diphenylpropanes, a new class of orally active GPBAR1 (TGR5) agonists

Henrietta Dehmlow [a,†], Rubén Alvarez Sánchez [b], Stephan Bachmann [a,‡], Caterina Bissantz [a], Fritz Bliss [a,‡], Karin Conde-Knape [c], Martin Graf [a], Rainer E. Martin [a], Ulrike Obst Sander [a], Susanne Raab [c], Hans G. F. Richter [a], Sabine Sewing [c], Urs Sprecher [c], Christoph Ullmer [c], Patrizio Mattei [a,*]

[a] Small Molecule Research, Pharma Research & Early Development (pRED), F. Hoffmann-La Roche AG, CH-4070 Basel, Switzerland
[b] Non-Clinical Safety, Pharma Research & Early Development (pRED), F. Hoffmann-La Roche AG, CH-4070 Basel, Switzerland
[c] Cardiovascular & Metabolism DTA, Pharma Research & Early Development (pRED), F. Hoffmann-La Roche AG, CH-4070 Basel, Switzerland

ARTICLE INFO

Article history:
Received 16 May 2013
Revised 6 June 2013
Accepted 8 June 2013
Available online 19 June 2013

Keywords:
GPBAR1
TGR5
PYY
GLP-1
Chemical probe

ABSTRACT

A series of non-steroidal GPBAR1 (TGR5) agonists was developed from a hit in a high-throughput screening campaign. Lead identification efforts produced biphenyl-4-carboxylic acid derivative (*R*)-**22**, which displayed a robust secretion of PYY after oral administration in a degree that can be correlated with the unbound plasma concentration. Further optimisation work focusing on reduction of the lipophilicity provided the 1-phenylpiperidine-4-carboxylic acid derivative (*R*)-**29** (RO5527239), which showed an improved secretion of PYY and GLP-1, translating into a significant reduction of postprandial blood glucose excursion in an oral glucose tolerance test in DIO mice.

The G-protein coupled bile acid receptor 1 (GPBAR1, also referred to as TGR5) has recently been identified as a mediator of several important metabolic processes in peripheral tissues.[1–4] Activated by bile acids at physiologically relevant concentrations and through Gαs stimulation, GPBAR1 elicits an intracellular increase of cAMP. In enteroendocrine cells, GPBAR1 activation has been shown to promote the secretion of several therapeutically relevant peptides, including the appetite regulating peptide YY (PYY) and the antihyperglycemic glucagon-like peptide 1 (GLP-1).

Whereas bile acids are also agonists of the farnesoid X receptor (FXR), a nuclear hormone receptor with a multitude of signalling functions for bile acid, lipid, and glucose metabolism,[5] several classes of selective agonists of the GPBAR1 have been developed in recent years, including the synthetic bile acid INT-777 (**1**, Fig. 1)[6] and a wide variety of non-steroidal compounds.[7–12] GPBAR1 agonists may complement the GLP-1 dependent therapeutic actions of antidiabetic medicines including dipeptidyl peptidase 4 inhibitors.[13] But in order to assess the pharmacological potential of GPBAR1 agonism there is a need for suitable, orally administered chemical probes,[14–16] which can be used to establish a plausible PK/PD relationship. We recently reported the discovery of a series of potent and selective, HTS-derived 2-phenoxy-nicotinamides with favourable in vitro properties, for example, **2** (Fig. 1).[17] Unfortunately, these compounds had poor pharmacokinetic properties in rodents and were therefore not suited for proof-of-concept studies in vivo. Here we present a set of structurally unrelated GPBAR1 agonists, which have culminated in well-behaved, orally bioavailable chemical probes.

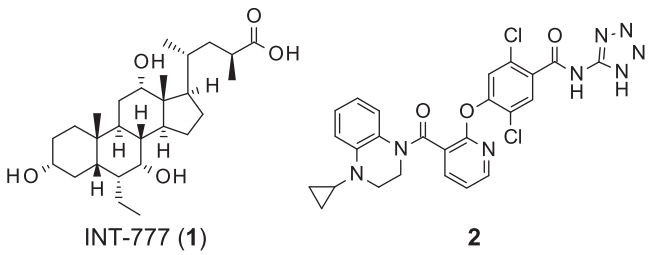

Figure 1. Selective GPBAR1 agonists.

* Corresponding author. Tel.: +41 68 6885438.
E-mail address: patrizio.mattei@roche.com (P. Mattei).
† Present address: Pharma Technical Regulatory, Pharma Global Technical Operations, F. Hoffmann-La Roche AG, CH-4070 Basel, Switzerland.
‡ Present address: Pharma Technical Development, Pharma Global Technical Operations, F. Hoffmann-La Roche AG, CH-4070 Basel, Switzerland.

0960-894X/$ - see front matter © 2013 Elsevier Ltd. All rights reserved.
http://dx.doi.org/10.1016/j.bmcl.2013.06.017

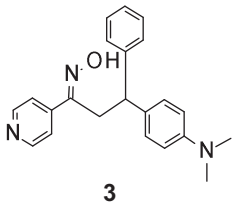

hGPBAR1, EC_{50} = 0.045 μM
mGPBAR1, EC_{50} = 2.0 μM
NCI-H716, EC_{50} = 2.9 μM
$logD_{7.4}$ = 3.4
solubility (pH 6.5): <1 mg/L
CYP3A4 IC_{50} <0.2 μM
mouse Cl_{mic} = 460 μL/min/mg

Figure 2. Profile of the HTS hit **3**.

Oxime **3** was identified in a high-throughput screening campaign of the corporate compound library. The compound was a full agonist with EC_{50} values of 45 nM and 2.0 μM at recombinant (CHO-expressed) human and mouse GPBAR1, respectively (Fig. 2). The compound also was able to stimulate cAMP production (EC_{50} = 2.9 μM) in the human intestinal enteroendocrine cell line NCI-H716, which endogenously expresses GPBAR1.[18] For comparison, the reference compound INT-777 (**1**) was less potent in this assay (EC_{50} = 13 μM). Oxime **3**, although stable in aqueous solution at pH 1–10 (>90% recovery after 2 h at 37 °C), suffered from poor physicochemical properties, such as high lipophilicity and poor aqueous solubility. Moreover, **3** was a sub-micromolar inhibitor of the CYP450 isoform 3A4.

Oxime **3** was prepared in a straightforward manner by 1,4-addition of benzeneboronic acid/diethylzinc[19] to the known azachalcone **4**,[20,21] followed by condensation of the ketone intermediate **5** with hydroxylamine (Scheme 1).[22] The isomeric oximes **3** and **6** could be separated by column chromatography. In comparison to (*E*)-oxime **3**, the (*Z*)-isomer **6** was about sixfold less active (EC_{50} = 0.27 μM), whereas the ketone intermediate **5** did not show any in vitro potency (EC_{50} > 10 μM).

Some initial SAR data around the HTS hit **3** are shown in Table 1. Oxime O-methylation is not tolerated (compound **7**), nor is replacement of the 4-pyridyl head group by 2- or 3-pyridyl, phenyl, or 4-fluorophenyl (compounds **8**–**11**). In contrast, the SAR around the phenyl substituent (R^2 in Table 1) is rather flat (compounds **12**–**15**), with an *ortho* methyl slightly enhancing the potency, whereas replacement of the phenyl by small alkyl groups such as ethyl is not tolerated (compound **16**).

The *o*-tolyl derivative **17** was used as a template for further evaluation (Table 2). Like the HTS hit **3**, compound **17** was a potent inhibitor of the CYP3A4 isoform, which is a well-known property of lipophilic *ortho*-unsubstituted pyridines.[23] The interaction with CYP3A4 could be disrupted by introduction of a methyl group next to the pyridine nitrogen without compromising the potency at the human GPBAR1 (**18**, EC_{50} = 28 nM). Alternatively, an *N*-methylpyridone head group was identified as a suitable bioisosteric replacement for the 2-methylpyridine (compound **19**, EC_{50} = 8 nM). To improve the drug-likeness of the highly lipophilic ($logD_{7.4}$ > 4) and metabolically unstable (mouse Cl_{mic} = 730 μL min^{-1} mg^{-1}) bromide **18**, various carboxylic acid derivatives were prepared (compounds **20**–**23**). Of these, *para*-substituted biphenylcarboxylic acid **22** was the most potent one and was chosen as lead compound for more extensive characterisation.

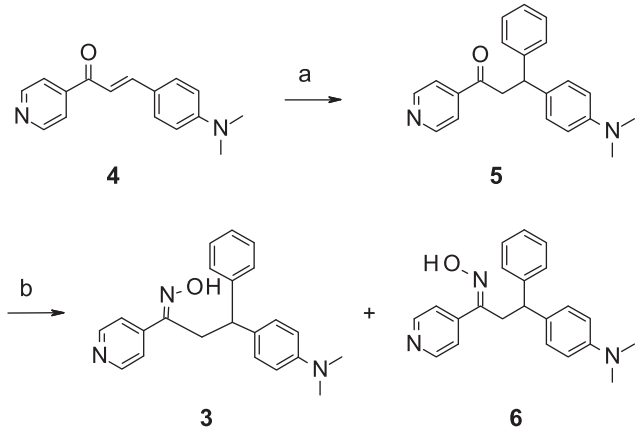

Scheme 1. Reagents and conditions: (a) $PhB(OH)_2$, Et_2Zn, toluene, 60 °C (62%); (b) $NH_2OH{\cdot}HCl$, NaOAc, EtOH, reflux (86%, *E*/*Z* ca. 6:1).

The individual enantiomers of **22** were obtained by preparative chiral HPLC separation, revealing that the (*R*)-enantiomer is about fivefold more potent than the (*S*)-enantiomer (Table 3).[24] For a more efficient access to enantiomerically pure compounds we devised a different synthetic route, which could be scaled up to multigram amounts (Scheme 2). Thus, 3,3-diarylpropionic acid **26**, which was produced in accordance with literature procedures,[25,26] was transformed into the Weinreb amide **27** under standard conditions.[27] This intermediate could be easily separated into its enantiomers (−)-(*R*)-**27** and (+)-(*S*)-**27** by preparative HPLC on a Chiralpak-AD column (1 kg scale).

For the synthesis of compounds with a 2-methylpyridin-4-yl head group, 4-bromo-2-methylpyridine was lithiated at −100 °C (the low temperature was necessary to minimise side reactions owing to the C–H acidity of the 2-picoline subunit) and reacted with **27**, leading to ketone **28**. Benzoic acid derivative **22** was obtained by Suzuki coupling[28,29] of **28** with 4-carboxybenzeneboronic acid, followed by reaction of the coupling product with hydroxylamine and acidic equilibration towards the thermodynamically more stable (*E*)-stereoisomer. Piperidine-4-carboxylic acid derivative **29** was produced from **28** by Buchwald–Hartwig amination[30] with ethyl piperidine-4-carboxylate, followed by ester hydrolysis, oxime formation, and acidic equilibration.

The synthesis of compounds with a 1-methyl-2-oxopyridin-5-yl head group started from 5-bromo-2-methoxypyridine, which after halogen–lithium exchange was reacted with Weinreb amide **27**, followed by acidic ether cleavage and methylation of the pyridone nitrogen, leading to ketone intermediate **30**. The (*Z*)- to (*E*)-equilibration of oximes **22** and **29** likely involves protonation of the basic pyridine nitrogen, which pyridones **31** and **32** are devoid of; therefore the synthetic sequence had to be slightly adapted. For benzoic acid **31**, ketone **30** was first transformed into the corresponding oxime, which after selective precipitation of the desired (*E*)-isomer from ethyl acetate was coupled with 4-carboxybenzeneboronic acid. Methylsulfone **32** was produced from **30** by a copper(I)-catalysed process using sodium methanesulfinate,[31] followed by oxime formation and HPLC separation from the undesired (*Z*)-isomer.

Biphenyl-4-carboxylic acid (*R*)-**22** was a potent agonist both at the mouse and human GPBAR1 (Table 3), whereas it was inactive in the FXR transactivation assay.[32,33] The submicromolar potency was also preserved in NCI-H716 cells, displaying a high efficacy relative to lithocholic acid. In comparison with the HTS hit **3**, lipophilicity is lower, which results in appreciable aqueous solubility. Likewise, the reduced microsomal clearance of (*R*)-**22** translates into a favourable PK in mice with high bioavailability.

The high exposure of (*R*)-**22** is paralleled by sustained PYY secretion in C57Bl/6 mice, reaching plasma concentrations that are significantly above the baseline levels of 100–200 pg mL^{-1} after a single oral dose of 50 or 100 mg kg^{-1}. Figure 3 illustrates the plasma concentration–effect relationship of (*R*)-**22** determined at various time points (0.1 h < *t* < 25 h). The timing of maximal plasma levels for (*R*)-**22** and PYY suggests a direct response mechanism systemically mediated. When corrected by these plasma binding effects (plasma free fraction about 0.2%), the in vitro EC_{50} of 140 nM translates into a total plasma exposure of about 31,500 ng mL^{-1}. The intravenous dose at 2 mg kg^{-1} showed only a trend for increased PYY secretion at the highest exposures, in line with the lower plasma levels achieved through this route.

Table 1
In vitro activity data for oximes **7–16** produced according to Scheme 1

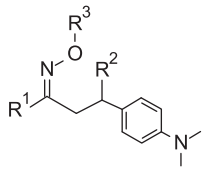

Compd	R^1	R^2	R^3	hGPBAR1 EC_{50}[a] (μM)	mGPBAR1 EC_{50}[a] (μM)	NCI -H716 EC_{50}[b] (μM)
7	Pyridin-4-yl	Phenyl	CH_3	>10 (9)		
8	Phenyl	Phenyl	H	>10 (19)		
9	4-F-phenyl	Phenyl	H	>10 (42)		
10	Pyridin-3-yl	Phenyl	H	>10 (19)		
11	Pyridin-2-yl	Phenyl	H	>10 (17)		
12	Pyridin-4-yl	2-CH_3-phenyl	H	0.025 (124)	0.70 (150)	1.04 (127)
13	Pyridin-4-yl	3-CH_3-phenyl	H	0.079 (69)	1.5 (202)	2.75 (74)
14	Pyridin-4-yl	4-CH_3-phenyl	H	0.1 (155)	1.1 (136)	
15	Pyridin-4-yl	Pyridin-2-yl	H	0.38 (144)	1.6 (115)	
16	Pyridin-4-yl	Ethyl	H	>10 (56)		

[a] EC_{50} values are the average of determinations performed in triplicate. For experimental details see Ref. 22. Values in parentheses are the efficacies (%) measured as maximum response relative to the response by stimulation with 10 μM lithocholic acid.
[b] EC_{50} values are the average of determinations performed in triplicate, values in parentheses are the efficacies (%) measured as maximum response relative to the response by stimulation with 10 μM lithocholic acid. For experimental details see Ref. 37.

Table 2
In vitro profiling data for oximes **17–23**

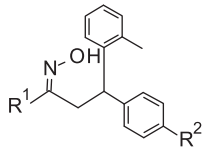

Compd	R^1	R^2	hGPBAR1, EC_{50}[a] (μM)	mGPBAR1, EC_{50}[a] (μM)	NCI -H716 EC_{50}[b] (μM)	CYP3A4 IC_{50}[c] (μM)
17	Pyridin-4-yl	Br	0.012 (124)	0.31 (99)	0.88 (102)	<0.2
18	2-CH_3-Pyridin-4-yl	Br	0.028 (93)	0.74 (97)	0.50 (106)	5.0
19	1-Methyl-2-oxopyridin-5-yl	Br	0.008 (105)	1.42 (250)	0.17 (104)	>50
20	2-CH_3-pyridin-4-yl	COOH	0.26 (89)	3.7 (109)		>50
21	2-CH_3-pyridin-4-yl	CH_2COOH	0.70 (89)	6.1 (87)		>50
22	2-CH_3-pyridin-4-yl	4-Carboxyphenyl	0.02 (81)	0.093 (123)	0.58 (131)	>50
23	2-CH_3-pyridin-4-yl	3-Carboxyphenyl	0.29 (84)	0.86 (100)		>50

[a] EC_{50} values are the average of determinations performed in triplicate. For experimental details see Ref. 22. Values in parentheses are the efficacies (%) measured as maximum response relative to the response by stimulation with 10 μM lithocholic acid.
[b] EC_{50} values are the average of determinations performed in triplicate, values in parentheses are the efficacies (%) measured as maximum response relative to the response by stimulation with 10 μM lithocholic acid. For experimental details see Ref. 37.
[c] CYP3A4 inhibitory potency determined by incubation in human liver microsomes using midazolam as substrate.

Table 3
In vitro/in vivo profiling data for advanced compounds

Cpd.	hGPBAR1 EC_{50}[a] (μM)	mGPBAR1 EC_{50}[a] (μM)	NCI-H716 EC_{50}[b] (μM)	log $D_{7.4}$[c]	Solubility (pH 6.5)[d]	Cl_{mic}[e]	Mouse pharmacokinetic parameters				f_u[k] (%)
							Cl[f,g]	V_{ss}[h,g]	$t^{1/2}$[i,g]	F (dose)[j]	
(*R*)-**22**	0.011 (100)	0.14 (145)	0.36 (192)	2.7	9	70	15	0.5	0.3	80 (23)	0.2
(*S*)-**22**	0.057 (95)	0.19 (167)	1.6 (124)	2.7	4	22					
(*R*)-**29**	0.004 (102)	0.028 (163)	0.08 (255)	1.5	270	13	5	0.4	1.7	100 (30)	1.9
(*S*)-**29**	0.023 (83)	0.13 (174)	0.75 (300)	1.6	230	22					
(*R*)-**31**	0.06 (102)	0.45 (151)	2.0 (115)	1.3	250	15	5	0.5	0.7	67 (49)	0.4
(*S*)-**31**	0.32 (93)	0.62 (183)	6.4 (92)	1.5	230	4					
(*R*)-**32**	0.026 (95)	1.3 (125)	0.46 (104)	1.7	300	58	67	3.3	2.2	29 (22)	11
(*S*)-**32**	0.08 (95)	3.0 (116)	1.4 (175)	1.9	240	84					

[a] EC_{50} values are the average of determinations performed in triplicate, for experimental details see Ref. 22. Values in parentheses are the efficacies (%) measured as maximum response relative to the response by stimulation with 10 μM lithocholic acid.
[b] EC_{50} values are the average of determinations performed in triplicate, values in parentheses are the efficacies (%) measured as maximum response relative to the response by stimulation with 10 μM lithocholic acid. For experimental details see Ref. 37.
[c] Distribution coefficient at pH 7.4; for experimental details see Ref. 38.
[d] Kinetic solubility, (mg L^{-1}).
[e] Clearance in mouse microsomes (c = 1 μM, 0.5 mg/mL protein), (μL min^{-1} mg^{-1}).
[f] Clearance, (mL min^{-1} kg^{-1}).
[g] Dose: 1 mg kg^{-1} iv.
[h] Volume of distribution at steady state, (L kg^{-1}).
[i] Half-life, (h).
[j] Oral bioavailability, (%); (dose, (mg kg^{-1})).
[k] Free fraction in mouse plasma.

The high exposures and doses required for a PYY response in vivo suggest that the activity of (*R*)-**22** is limited by the low free fraction, which is characteristic for lipophilic carboxylic acids.[34] Therefore, optimisation of (*R*)-**22** focused on reduction of the lipophilicity (log $D_{7.4}$) and/or replacement of the carboxylic acid by a polar uncharged group.

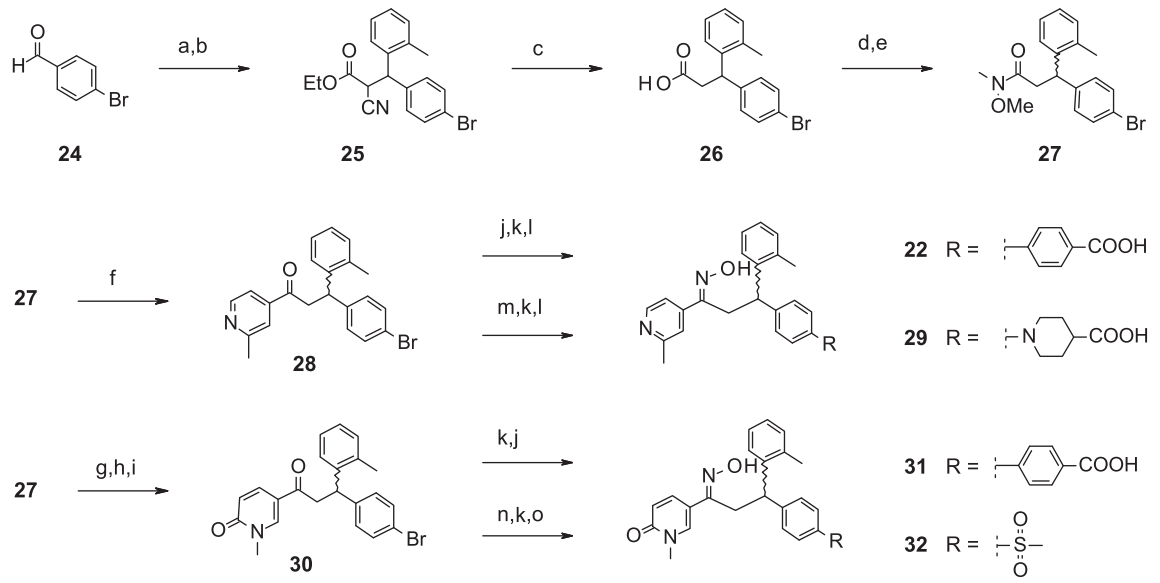

Scheme 2. Reagents and conditions: (a) ethyl cyanoacetate, morpholine, reflux (87%); (b) *o*-tolylmagnesium chloride, 2-methyltetrahydrofuran, rt (quant.); (c) HOAc, H_2SO_4, 15 h, 110 °C (72%); (d) HNMe(OMe)·HCl, TBTU, Et_3N, DMF (91%); (e) Reprosil Chiral-NR, heptane/2-propanol 4:1 (46% (−)-(*R*)-**27** and 42% (+)-(*S*)-**27**); (f) 4-bromo-2-methylpyridine (2.5 equiv), *n*-BuLi (2.5 equiv), THF, −100 °C (70%); (g) 5-bromo-2-methoxypyridine (2.5 equiv), *n*-BuLi (2.5 equiv), THF, −78 °C (77%); (h) 37% aq HCl, 1,4-dioxane, 100 °C, 90 min (95%); (i) iodomethane, K_2CO_3, *N*,*N*-dimethylacetamide (80%); (j) 4-carboxybenzeneboronic acid, $PdCl_2$(dppf), aq Na_2CO_3, 1,4-dioxane (73–82%); (k) NH_2OH·HCl, NaOAc, aq EtOH, reflux (50–95%); (l) HCl, 1,4-dioxane or DME; (m) ethyl piperidine-4-carboxylate, $Pd_2(dba)_3$ (0.05 equiv), X-Phos (0.05 equiv), NaO*t*Bu, toluene, 85 °C, then LiOH, H_2O (76%); (n) sodium methanesulfinate, L-proline, NaOH, CuI, DMSO (93%); (o) Chiralpak-AD, heptane/ethanol 3:2 (70%).

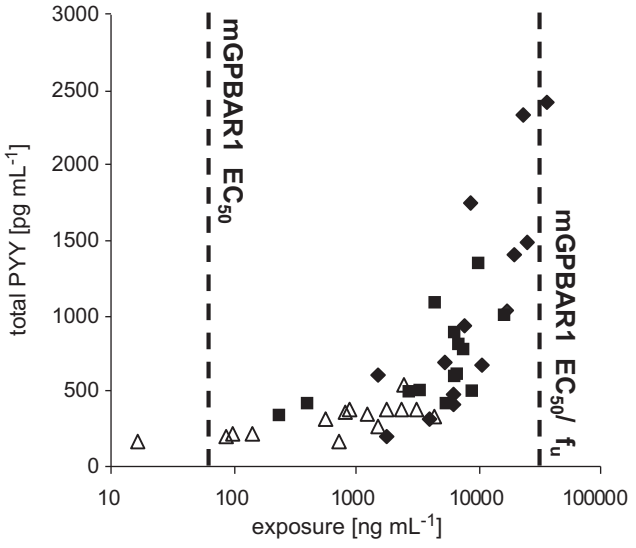

Figure 3. Plasma concentrations of total PYY (*y*-axis) and (*R*)-**22** (*x*-axis) at various time points after administration of (*R*)-**22** at 100 mg kg^{-1} po (♦), 50 mg kg^{-1} po (■), or 2 mg kg^{-1} iv (△), in C57Bl/6 DIO mice. The vertical dashed lines correspond to the EC_{50} of (*R*)-**22** at the mouse GPBAR1 (140 nM ≡ 63 ng mL^{-1}) and to the plasma binding corrected mouse EC_{50} of (*R*)-**22** (63 ng mL^{-1}/f_u = 31,500 ng mL^{-1}, with f_u = 0.002).

The lipophilicity may be reduced by replacement of the 2-methylpyridin-4-yl head group with 1-methyl-2-oxopyridin-5-yl, as already evidenced by compound **19**. Indeed, biphenyl-4-carboxylic acid (*R*)-**31** is more than one order of magnitude less lipophilic than (*R*)-**22**, but its free fraction is only slightly higher and does not fully compensate for the lower activity at the target. Also, the pharmacokinetic properties in mice are not significantly improved in comparison with (*R*)-**22**, despite a lower clearance in vivo (Table 3).

Replacement of the carboxyphenyl subunit of (*R*)-**31** by a methylsulfonyl group resulted in compound (*R*)-**32**, which is roughly equipotent to (*R*)-**31** and also comparable in terms of lipophilicity and solubility. As anticipated (*R*)-**32** has a significantly higher free fraction (11%), but the rather poor pharmacokinetic properties due to high clearance and low oral bioavailability (C_{max} = 870 ng mL^{-1} at 22 mg kg^{-1} po) precluded any further consideration of this compound (Table 3).

The piperidine-carboxylic acid derivative (*R*)-**29** was selected as the chemical probe of choice. (*R*)-**29** is the most potent compound of this series both at recombinant mouse and human GPBAR1 as well as in NCI-H716 cells (Table 3). (*R*)-**29** is only moderately lipophilic (log$D_{7.4}$ = 1.5) and reasonably soluble (270 mg L^{-1} at pH 6.5). In comparison to (*R*)-**22**, (*R*)-**29** has a 10-fold higher free fraction and more favourable pharmacokinetic properties in mouse most likely due to lower clearance (C_{max} = 41,000 ng mL^{-1} at 30 mg kg^{-1} po).

Similar to (*S*)-**22**, the enantiomeric compounds (*S*)-**29**, (*S*)-**31**, and (*S*)-**32** were somewhat less potent than the respective (*R*)-enantiomers (Table 2).

Compounds (*R*)-**29** and (*R*)-**22** were tested in an oral glucose tolerance test in GPBAR1-KI mice—mice that express human GPBAR1 instead of mouse GPBAR1.[35] In this experiment, (*R*)-**29** administered orally 2 h before the glucose challenge at 10 or 30 mg kg^{-1} as well (*R*)-**22** at 100 mg kg^{-1} produced an approximately 30% decrease in postprandial glucose excursion (AUC_{0-120}, area under the curve, 0 → 120 min). Meanwhile, plasma PYY and GLP-1 levels were markedly increased in all treatment groups, with (*R*)-**29** at 10 mg kg^{-1} being similarly efficient as (*R*)-**22** at 100 mg kg^{-1} (Fig. 4). However, (*R*)-**29** was unsuitable for chronic administration because it was found to be an inducer of CYP3A4,[36] resulting in decreased systemic exposure over time.

In summary, we have discovered a new class of HTS-derived oxime derivatives. The starting point (**3**) was already fairly potent at the GPBAR1 but required improvement in terms of physicochemical properties. These efforts have delivered the highly selective,[35] moderately lipophilic, and orally bioavailable piperidine-4-carboxylic acid (*R*)-**29**, which acts as a strongly efficacious PYY/GLP-1 secretagogue and reduces postprandial blood glucose

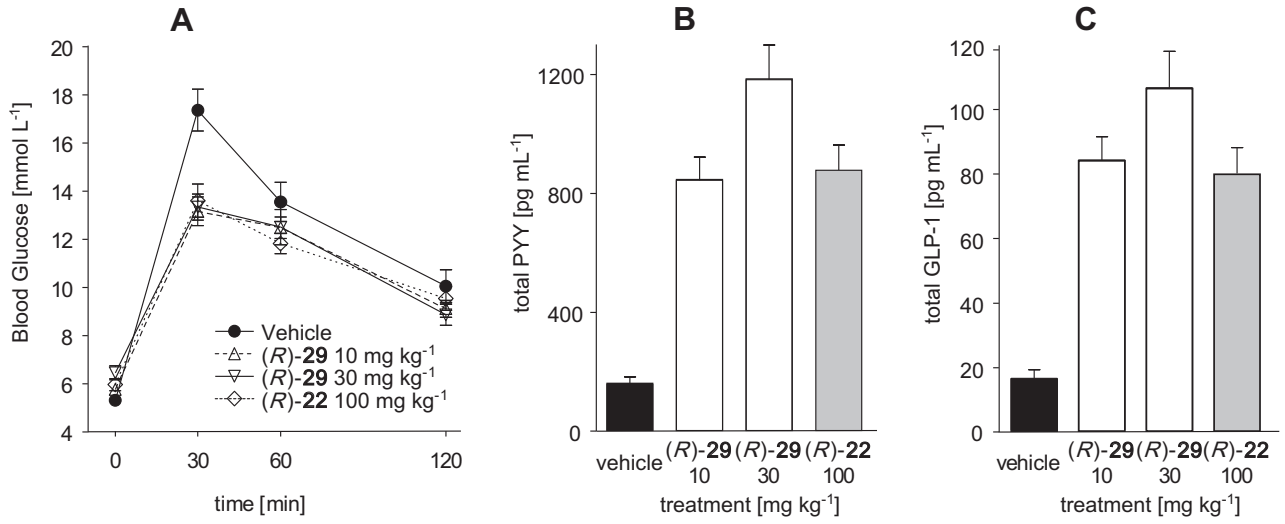

Figure 4. (A) Oral glucose tolerance test (2 g kg^{-1} glucose) in male 12 week old GPBAR1-KI mice [B6 Gpbar1∗tm1(GPBAR1)Ait] treated with vehicle ● (Klucel 2%, Tween 0.1%), (*R*)-**29** △ (10 mg kg^{-1}), (*R*)-**29** ▽ (30 mg kg^{-1}) or (*R*)-**22** ◇ (100 mg kg^{-1}). Animals were first dosed with compound or vehicle 60 min before glucose bolus. Data represent the mean ± S.E.M. (B) Plasma PYY levels measured in male 12 week old GPBAR1-KI mice [B6 Gpbar1∗tm1(GPBAR1)Ait][35] 60 min after oral treatment with vehicle (Klucel 2%, Tween 0.1%), (*R*)-**29** (10 mg kg^{-1}), (*R*)-**29** (30 mg kg^{-1}) or (*R*)-**22** (100 mg kg^{-1}). Data represent the mean ± S.E.M. (C) Plasma total GLP–1 levels measured in male 12 week old GPBAR1-KI mice [B6 Gpbar1∗tm1(GPBAR1)Ait] 60 min after oral treatment with vehicle (Klucel 2%, Tween 0.1%), (*R*)-**29** (10 mg kg^{-1}), (*R*)-**29** (30 mg kg^{-1}) or (*R*)-**22** (100 mg kg^{-1}). Data represent the mean ± S.E.M.

levels in mice. An in-depthaccount of the biochemistry and pharmacology of (*R*)-**29** (RO5527239) is presented in a separate paper.[35]

Acknowledgments

The authors gratefully acknowledge Michel Altermatt, Manuela Baumann, Anne-Sophie Cuvier, Patrick Di Giorgio, Olivier Gavelle, Selina Hodel, Marie-Paule Imhoff, Kersten Klar, Michel Lindemer, Noemi Raschetti, Flore Reggiani, Martin Ritter, Marianne Rueher, Joana Salta, Petra Schmitz, Kurt Schönbächler, Regi Schöttli, and Jitka Weber for chemical syntheses, Ernst Kupfer, Jacky Joerger and Daniel Zimmerli for preparative HPLC separations, Tanja Minz, Anja Osterwald, Astride Schnoebelen, Vera Griesser and Angelina Waller for in vitro biological testing, Stefan Masur and Isabelle Walter for bioanalytics, Isabelle Parrilla, Yves Siegrist, Sandrine Simon, Volkmar Starke and Björn Wagner for in vitro ADME measurements, and Wolfgang Rapp for in vivo experiments.

References and notes

1. Pols, T. W. H.; Noriega, L. G.; Nomura, M.; Auwerx, J.; Schoonjans, K. *J. Hepatol.* **2011**, *54*, 1263.
2. Thomas, C.; Gioiello, A.; Noriega, L.; Strehle, A.; Oury, J.; Rizzo, G.; Macchiarulo, A.; Yamamoto, H.; Mataki, C.; Pruzanski, M.; Pellicciari, R.; Auwerx, J.; Schoonjans, K. *Cell Metab.* **2009**, *10*, 167.
3. Pols, T. W. H.; Nomura, M.; Harach, T.; Lo Sasso, G.; Oosterveer, M. H.; Thomas, C.; Rizzo, G.; Gioiello, A.; Adorini, L.; Pellicciari, R.; Auwerx, J.; Schoonjans, K. *Cell Metab.* **2011**, *14*, 747.
4. Parker, H. E.; Wallis, K.; Le Roux, C. W.; Wong, K. Y.; Reimann, F.; Gribble, F. M. *Br. J. Pharmacol.* **2012**, *165*, 414.
5. Thomas, C.; Pellicciari, R.; Pruzanski, M.; Auwerx, J.; Schoonjans, K. *Nat. Rev. Drug Disc.* **2008**, *7*, 678.
6. Pellicciari, R.; Gioiello, A.; Macchiarulo, A.; Thomas, C.; Rosatelli, E.; Natalini, B.; Sardella, R.; Pruzanski, M.; Roda, A.; Pastorini, E.; Schoonjans, K.; Auwerx, J. *J. Med. Chem.* **2009**, *52*, 7958.
7. Xu, Y. *Annu. Rep. Med. Chem.* **2011**, *46*, 69.
8. Gioiello, A.; Rosatelli, E.; Nuti, R.; Macchiarulo, A.; Pellicciari, R. *Expert Opin. Ther. Pat.* **2012**, *22*, 1399.
9. Duan, H.; Ning, M.; Chen, X.; Zou, Q.; Zhang, L.; Feng, Y.; Zhang, L.; Leng, Y.; Shen, J. *J. Med. Chem.* **2012**, *55*, 10475.
10. Piotrowski, D. W.; Futatsugi, K.; Warmus, J. S.; Orr, S. T. M.; Freeman-Cook, K. D.; Londregan, A. T.; Wei, L.; Jennings, S. M.; Herr, M.; Coffey, S. B.; Jiao, W.; Storer, G.; Hepworth, D.; Wang, J.; Lavergne, S. Y.; Chin, J. E.; Hadcock, J. R.; Brenner, M. B.; Wolford, A. C.; Janssen, A. M.; Roush, N. S.; Buxton, J.; Hinchey, T.; Kalgutkar, A. S.; Sharma, R.; Flynn, D. A. *ACS Med. Chem. Lett.* **2013**, *4*, 63.
11. Futatsugi, K.; Bahnck, K. B.; Brenner, M. B.; Buxton, J.; Chin, J. E.; Coffey, S. B.; Dubins, J.; Flynn, D.; Gautreau, D.; Guzman-Perez, A.; Hadcock, J. R.; Hepworth, D.; Herr, M.; Hinchey, T.; Janssen, A. M.; Jennings, S. M.; Jiao, W.; Lavergne, S. Y.; Li, B.; Li, M.; Munchhof, M. J.; Orr, S. T. M.; Piotrowski, D. W.; Roush, N. S.; Sammons, M.; Stevens, B. D.; Storer, G.; Wang, J.; Warmus, J. S.; Wei, L.; Wolford, A. C. *MedChemCommun* **2013**, *4*, 205.
12. Londregan, A. T.; Piotrowski, D. W.; Futatsugi, K.; Warmus, J. S.; Boehm, M.; Carpino, P. A.; Chin, J. E.; Janssen, A. M.; Roush, N. S.; Buxton, J.; Hinchey, T. *Bioorg. Med. Chem. Lett.* **2013**, *23*, 1407.
13. Drucker, D. J.; Nauck, M. A. *Lancet* **2006**, *368*, 1696.
14. Lipinski, C. A. *Drug Discovery Today: Technol.* **2004**, *1*, 337.
15. Frye, S. V. *Nat. Chem. Biol.* **2010**, *6*, 159.
16. Bunnage, M. E.; Chekler, E. L. P.; Jones, L. H. *Nat. Chem. Biol.* **2013**, *9*, 195.
17. Martin, R. E.; Bissantz, C.; Gavelle, O.; Kuratli, C.; Dehmlow, H.; Richter, H. G. F.; Obst Sander, U.; Erickson, S. D.; Kim, K.; Pietranico-Cole, S. L.; Alvarez-Sanchez, R.; Ullmer, C. *ChemMedChem* **2013**, *8*, 569.
18. Maruyama, T.; Miyamoto, Y.; Nakamura, T.; Tamai, Y.; Okada, H.; Sugiyama, E.; Nakamura, T.; Itadani, H.; Tanaka, K. *Biochem. Biophys. Res. Commun.* **2002**, *298*, 714.
19. Dong, L.; Xu, Y.-J.; Gong, L.-Z.; Mi, A.-Q.; Jiang, Y.-Z. *Synthesis* **2004**, 1057.
20. Krasnec, L.; Durinda, J.; Szucs, L. *Chem. Zvesti* **1961**, *15*, 558.
21. Annigeri, A. C.; Siddappa, S. *Indian J. Chem.* **1963**, *1*, 484.
22. Bissantz, C.; Dehmlow, H.; Erickson, S. D.; Kim, K.; Martin, R. E.; Mattei, P.; Obst Sander, U.; Pietranico-Cole, S. L.; Richter, H.; Ullmer, C. U.S. Pat. Appl. 0,010,190, 2012.
23. Zlokarnik, G.; Grootenhuis, P. D. J.; Watson, J. B. *Drug Discovery Today* **2005**, *10*, 1443.
24. The assignment of the absolute configuration of the enantiomers was based on the X-ray crystal structure of (*S*)-2-({4′-[(*S*)-3-(2-methyl-pyridin-4-yl)-3-oxo-1-*o*-tolyl-propyl]-biphenyl-4-carbonyl}-amino)-propionic acid (Ref. 22), the L-alanine amide conjugate of the ketone precursor of (*S*)-**22**.
25. Boegesoe, K. P. *J. Med. Chem.* **1983**, *26*, 935.
26. Gu, X.-H.; Yu, H.; Jacobson, A. E.; Rothman, R. B.; Dersch, C. M.; George, C.; Flippen-Anderson, J. L.; Rice, K. C. *J. Med. Chem.* **2000**, *43*, 4868.
27. Nahm, S.; Weinreb, S. M. *Tetrahedron Lett.* **1981**, *22*, 3815.
28. Gong, Y.; Pauls, H. W. *Synlett* **2000**, 829.
29. Magano, J.; Dunetz, J. R. *Chem. Rev. (Washington, DC, US)* **2011**, *111*, 2177.
30. Huang, X.; Anderson, K. W.; Zim, D.; Jiang, L.; Klapars, A.; Buchwald, S. L. *J. Am. Chem. Soc.* **2003**, *125*, 6653.
31. Zhu, W.; Ma, D. *J. Org. Chem.* **2005**, *70*, 2696.
32. Kanaya, E.; Shiraki, T.; Jingami, H. *Biochem. J.* **2004**, *382*, 913.
33. Richter, H. G. F.; Benson, G. M.; Blum, D.; Chaput, E.; Feng, S.; Gardes, C.; Grether, U.; Hartman, P.; Kuhn, B.; Martin, R. E.; Plancher, J.-M.; Rudolph, M. G.; Schuler, F.; Taylor, S.; Bleicher, K. H. *Bioorg. Med. Chem. Lett.* **2011**, *21*, 191.
34. Fessey, R. E.; Austin, R. P.; Barton, P.; Davis, A. M.; Wenlock, M. C. In *Pharmacokinetic Profiling in Drug Research*; Testa, B., Krämer, S. D., Wunderli-Allenspach, H., Folkers, G., Eds.; Verlag Helvetica Chimica Acta: Zürich, 2006; pp 119–141.

35. Ullmer, C.; Alvarez Sanchez, R.; Sprecher, U.; Raab, S.; Mattei, P.; Dehmlow, H.; Sewing, S.; Iglesias, A.; Beauchamp, J.; Conde-Knape, K. *Br. J. Pharmacol.* **2013**, *169*, 671.
36. Fahmi, O. A.; Kish, M.; Boldt, S.; Obach, R. S. *Drug Metab. Dispos.* **2010**, *38*, 1605.
37. Subclone, NCI-H716#32, was identified by limited dilutions for optimised GPBAR1-dependent cAMP responses. cAMP was measured as described in Ref. 35 with the following modifications. Cells (10^5 cells per well) were seeded 17–24 h prior to the experiment in a black, poly-D-lysine coated 96 well plate with clear bottom (BD Biosciences, Heidelberg, Germany) in growth medium (RPMI-1640) with 10% FBS. One hour later each well received 5 mM sodium butyrate.
38. Bendels, S.; Kansy, M.; Wagner, B.; Huwyler, J. *Eur. J. Med. Chem.* **2008**, *43*, 1581.